

Interaction in the dark sector

Sergio del Campo* and Ramón Herrera†

*Instituto de Física, Pontificia Universidad Católica de Valparaíso,
Av. Universidad 330, Campus Curauma, Valparaíso, Chile*

Diego Pavón‡

*Departamento de Física, Universidad Autónoma de Barcelona,
08193 Bellaterra (Barcelona), Spain*

It may well happen that the two main components of the dark sector of the Universe, dark matter and dark energy, do not evolve separately but interact nongravitationally with one another. However, given our current lack of knowledge on the microscopic nature of these two components there is no clear theoretical path to determine their interaction. Yet, over the years, phenomenological interaction terms have been proposed on mathematical simplicity and heuristic arguments. In this paper, based on the likely evolution of the ratio between the energy densities of these dark components, we lay down reasonable criteria to obtain phenomenological, useful, expressions of the said term independent of any gravity theory. We illustrate this with different proposals which seem compatible with the known evolution of the Universe at the background level. Likewise, we show that two possible degeneracies with noninteracting models are only apparent as they can be readily broken at the background level. Further, we analyze some interaction terms that appear in the literature.

PACS numbers:

PACS: 98.80.-k, 95.35.+d, 95.36.+x

I. INTRODUCTION

Usually the present Universe is described by the Friedmann-Robertson-Walker (FRW) metric coupled to the dominant energy components, viz. baryons, dark matter (DM), and dark energy (DE). The two first constitute the main ingredients of cosmic structure. The latter two comprise the so-called “dark sector” as their presence is felt only by their gravitational interaction with the former. While DM (alongside the baryons) is nearly pressureless, DE is endowed with a high negative pressure responsible for the present accelerated expansion. Since, thus far, the information available on these two components is indirect —they have never been directly detected, much less produced in the lab — their nature remains unveiled. This may explain the very often minimalist assumption that they evolve independently of each other, i.e., that they interact with one another (and with whatever other component) gravitationally only. Nevertheless, there is no reason *a priori* why they should absolutely not interact otherwise; further, a coupling in the dark sector is not only natural, it seems inevitable [1]-[5].

The simplest cosmological model with a high degree of success from the observational side [the so-called lambda cold dark matter (ΛCDM)] takes as DE component the cosmological constant, or what is dynamically equivalent, the energy density of the quantum vacuum though finely tuned to a tiny value. Alongside this tuning problem it also presents the so-called “coincidence problem”, i.e., the fact that nowadays the energy density of DM is of the same order as that of the cosmological constant despite the former declines with cosmic expansion as a^{-3} (where a is the scale factor of the FRW metric) while the latter remains fixed [6].

A way to alleviate, or even solve, the latter problem is to allow for some nongravitational interaction in the dark sector that gives rise to a continuous transfer of energy from DE to DM. (Note that a transfer in the opposite direction would only exacerbate the problem, so it is more appealing to assume that the transfer occurs just in that sense; although the opposite possibility is not excluded, neither is the possibility of one or more changes in the direction of the transfer as the Universe expands). Current data are compatible with such transfer although the evidence is, so far, not fully conclusive [7–9]. For reviews on the subject see [10, 11] and references therein. See, also,

* Deceased

† E-mail: ramon.herrera@ucv.cl

‡ E-mail: diego.pavon@uab.es

the recent contributions [12, 13].

Given our ignorance about the nature of the components of the dark sector (to begin with, we do not even know whether these are single or multiple components), there is no reliable guidance to determine the interaction term. Therefore, the expressions proposed in the literature (except for the obvious restriction that such term must be small, not to deviate seriously from the predictions of the Λ CDM model) are necessarily phenomenological and based on heuristic arguments. Here we propose a different route to arrive at reasonable expressions of such term based on the likely evolution of the ratio between the densities of DM and DE.

From the history of structure formation we know that the former dominated at early times (though preceded by a short period of radiation prevalence), and from the current accelerated expansion we infer that the latter started to dominate in the recent past, and it will likely dominated for ever—at least if the Λ CDM or a slight variant of it turns to be the right cosmological model. Therefore, qualitatively speaking, the said ratio must decrease monotonously for most of the time. Although, as argued below, at very high redshifts it must have varied little or even stayed constant, and it will also scarcely vary or be constant in the far future. Accordingly, by wisely parametrizing the said ratio and using the conservation equations of the energy components, valid in most theories of gravity, compelling expressions for the interaction term are readily obtained.

This paper is organized as follows. Section II relates the interaction term with the said ratio, establishes the criteria that any reasonable parametrization of the latter should comply with and illustrates it by proposing three different parametrizations based solely on the FRW metric and the energy conservation equations. Section III makes use of recent data on the Hubble history to constrain the free parameters entering these parametrizations. Section IV deals with two apparent degeneracies between the interaction term and the equation of state (EOS) of DE. Section V considers different proposals for the interaction term made in the literature to see whether their corresponding ratios between the energy densities comply with the criteria of SEc. II. Finally, Sec. VI summarizes our findings.

As usual, a subscript zero attached to any quantity means that the latter is to be evaluated at present time.

II. PARAMETRIZING THE RATIO DM/DE

Let us consider a homogeneous and isotropic universe whose main energy components are baryons, dark matter and dark energy, subscripts b , m , and x , respectively. The first two being pressureless, the latter with a not necessarily constant EOS parameter $w = p_x/\rho_x < -1/3$.

We first look for an equation describing the dependence of the quantity, Q , that gauges the strength of the interaction in the dark sector, on the ratio between the densities of DM and DE, $r \equiv \rho_m/\rho_x$. Thus, we write the conservation equations of the components as

$$\dot{\rho}_b + 3H\rho_b = 0, \quad (1)$$

$$\dot{\rho}_m + 3H\rho_m = Q, \quad (2)$$

$$\dot{\rho}_x + 3H(1+w)\rho_x = -Q, \quad (3)$$

where $H \equiv \dot{a}/a$ denotes the Hubble function. In writing last two equations we have implicitly assumed that all DM and all DE participate in the interaction. For $Q > 0$ energy flows from DE to DM and vice versa for Q featuring the opposite sign; however, as mentioned above, we will take $Q > 0$ as it alleviates the coincidence problem. In accordance with strong constraints from local gravity experiments [14, 15] we assumed that the baryons conserve separately.

As it is readily derived, the condition $Q \geq 0$ imposes $\dot{r}/r \geq 3Hw$, i.e., it restricts the rate at which r can decrease as the Universe expands. (Recall that in the Λ CDM model ($w = -1$) one has $\dot{r} = -3Hr$).

From the above, we get

$$Q = \left(\frac{a r'}{r} - 3w \right) H \frac{\rho_m}{1+r}, \quad (4)$$

where the prime stands for d/da .

We reasonably expect Q to be smaller than the second term on the left-hand side of (2). This, alongside the restriction $Q > 0$, leads to $0 < ar' - 3wr < 3(r + r^2)$.

We now look for reasonable expressions for r to be inserted in (4); this, by passing, will illustrate our method. Any expression for r should satisfy $dr/da < 0$, except when $a \rightarrow 0$ and when $a \rightarrow \infty$, because in these limits r must either state constant or vary very slowly. Hence the quantities $r_+ \equiv r(a \rightarrow 0)$, $r_0 \equiv r(a = 1) \simeq 25/70$,¹ and $r_- \equiv r(a \rightarrow \infty)$ must fulfill $0 \leq r_- < r_0 < 1 < r_+$, with r_+ finite. Should the latter diverge, it would be because of one of the three following possibilities: (i) ρ_x vanished and ρ_m stayed finite as $a \rightarrow 0$. Then, the initial amount of DE would be zero and no transfer of DE to DM could ever occur whence Q would vanish altogether at all times. (ii) ρ_x remained bounded but ρ_m diverged (in the same limit as above). In this second case Eq. (2) implies that Q would diverge, and by (3) $\dot{\rho}_x$ would become minus infinity. This, in turn, would lead to the instantaneous transfer of the total amount of DE to DM. That is to say, the dark energy component would disappear completely for good. However, if ρ_m would obey $\rho_m = \text{constant } a^{-3} + \epsilon(a)$ where ϵ does not vanish as $a \rightarrow 0$, things would be different, because in this instance, Q does not diverge. This introduces an extra uncoupled DM parameter that could be included when comparing with the data. Nevertheless, the expression for ρ_m corresponds to the case where not all DM interacts, only a part of the total, but this was already excluded from our assumptions above. (iii) Both energy densities diverge, but ρ_m tends to a higher infinity than ρ_x does. Clearly, this case is the same as the previous one. Finally, the expression for r must gently interpolate between r_+ and r_- . Observational data suggest that the former is much larger than unity; see, e.g., [16, 17].

The possibility that for some period between r_+ and r_0 the ratio r is not decreasing would imply a severe deviation from the Λ CDM model that, most likely, would bring observable consequences on structure formation and the integrated Sachs-Wolfe effect. This is why we assume that $dr/da < 0$, except possibly at r_+ and r_- .

A. First parametrization

A possible choice for the ratio ρ_m/ρ_x is

$$r = r_- + \frac{r_+ - r_-}{1 + \beta a^\alpha}, \quad (5)$$

where α and β are positive-definite constants. As it can be readily checked (5) complies with the above conditions, and the corresponding current ratio is $r_0 = r_- + (r_+ - r_-)(1 + \beta)^{-1}$. If, as it seems reasonable (at least for $w = \text{constant}$), $r_+ \gg r_-$, then $r_+ \simeq r_0(1 + \beta)$. This suggests $\beta \gg 1$.

From the condition $Q \geq 0$, it follows that $ar'/r > 3w$. This alongside the observationally well-supported assumption $r_+ \gg r_-$, yields

$$\frac{ar'}{r} \simeq -\frac{\alpha\beta a^\alpha}{1 + \beta a^\alpha} \geq 3w, \quad (6)$$

thereby in the limit $a \gg 1$, the constraint $\alpha \leq 3 |w|$ follows.

The first derivative of r , evaluated at present time ($a = 1$) and under the assumption $r_- \ll r_+$, yields

$$r'(a = 1) \simeq -r_0 \frac{\beta}{1 + \beta} \alpha \simeq -r_0 \alpha. \quad (7)$$

Because $0 \leq \alpha \leq 3$, it is seen that $|r'(a = 1)| \leq 3r_0$ whereby the slope of r at $a = 1$ is more gentle than the corresponding one of Λ CDM model, $3r_0$, whence the coincidence problem gets alleviated.

Figure 1 shows the evolution of r for some chosen values of the free parameters compatible with observational data, at least, at the background level.

In the particular but interesting case that $w = -1$ and $r_+ \gg r_-$ we have

$$Q \simeq \left(3 - \frac{\alpha\beta a^\alpha}{1 + \beta a^\alpha}\right) H \frac{1 + \beta a^\alpha}{r_+ + 1 + \beta a^\alpha} \rho_m. \quad (8)$$

¹ For simplicity, we take the current energy budget as: baryons 5%, DM 25%, and DE 70%.

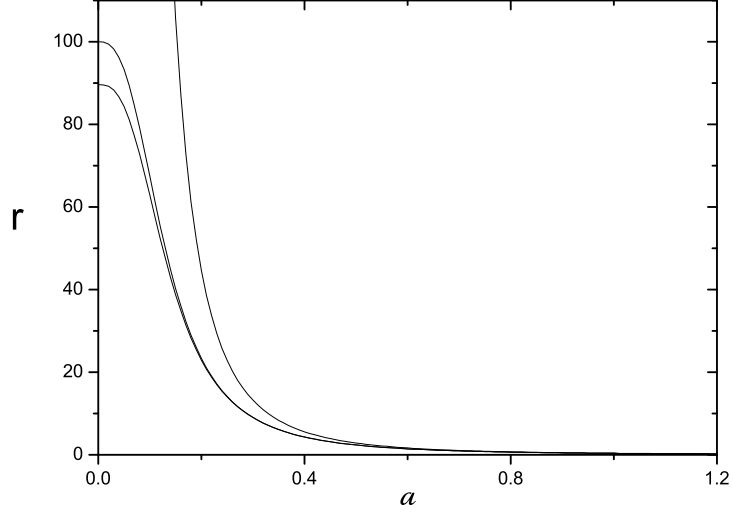


Figure 1: The first curve (from left to right) shows the evolution of ratio ρ_m/ρ_x corresponding to the expression (5) where we have used $\alpha = 2.70$ and $\beta = 89.6$, consequently $r_+ = 32.36$. The same can be said for the next curve but with $\alpha = 2.76$, $\beta = 279$, and $r_+ = 100$. The right-most curve depicts for comparison, the evolution of the ratio for the concordance Λ CDM model, $\rho_m/\rho_\Lambda = r_0 a^{-3}$. In all three cases, we have taken $r_0 = 25/70$. As it is apparent, the interaction $Q > 0$ mitigates the coincidence problem.

This illustrates how a reasonable expression for the interaction term between DM and DE can be devised from simple arguments based on the evolution of the ratio ρ_m/ρ_x .

By inserting the last expression in Eq. (2) we obtain, after integration, the evolution of the DM density,

$$\frac{\rho_m}{\rho_{m0}} = a^{-\frac{3r_+}{1+r_+}} \left[\frac{1+r_+ + \beta a^\alpha}{1+r_+ + \beta} \right]^{-\frac{\alpha(1+r_+) - 3r_+}{\alpha(1+r_+)}}. \quad (9)$$

In the limiting cases $a \ll 1$ and $a \rightarrow \infty$, one has $\rho_m \propto a^{-3r_+/(1+r_+)}$ and $\rho_m \propto a^{-\alpha}$, respectively. These results are very reasonable. At early times the interaction has not had much chance to be felt; besides, the second term on the left-hand side of (2) is much larger than Q , thereby the DM density goes down practically as if it were no interaction, $\rho_m \sim a^{-3}$. At late times, the interaction has had plenty of time to be felt and Q is not so small as compared with the said second term; thus ρ_m departs from the case of just pure expansion and goes down more slowly.

Figure 2 depicts, for illustrative purposes, the evolution of the ratios ρ_m/ρ_{m0} and ρ_x/ρ_{m0} for some selected values of the free parameters.

B. Second parametrization

Another possible expression for the ratio ρ_m/ρ_x is

$$r = r_- \exp\left(\frac{\lambda}{1+a}\right), \quad (10)$$

where $r_- = r(a \rightarrow \infty) > 0$ and $\lambda > 0$. On the other hand, $r_+ \equiv r(a \rightarrow 0) = r_0 e^{\lambda/2}$; see Fig. 3 for the cases $\lambda = 8$ and 10, both with $r_0 = 25/70$.

The condition for alleviating the coincidence problem $|r'(a=1)| < 3r_0$ implies $\lambda < 12$. For $w = -1$, this upper

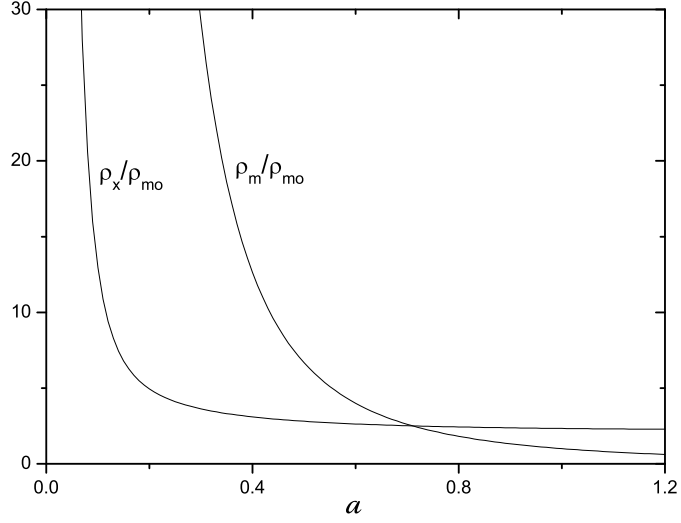


Figure 2: The curve on the right specializes Eq. (9) for $\alpha = 2.5$, $r_+ = 100$, and $\beta = 697/3$. The curve on the left results from dividing the previous one by r , as given by Eq. (5).

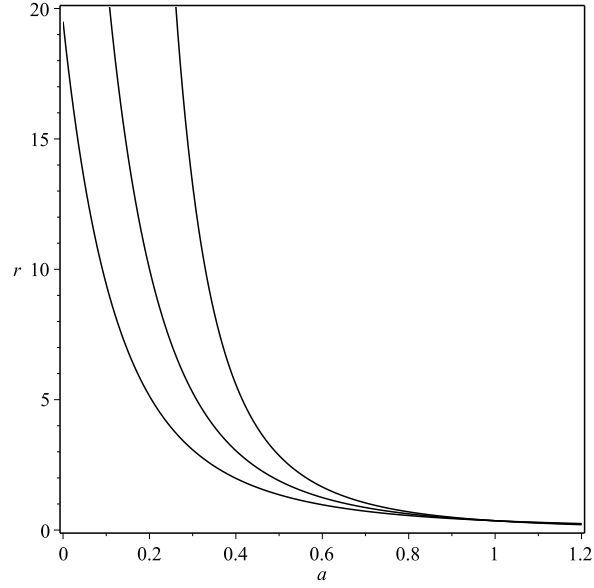


Figure 3: The first two curves from left to right, with $\lambda = 8$ and 10 , respectively, and $r_0 = 25/70$, depict the ratio ρ_m/ρ_x described by Eq. (10). Though not apparent in the figure these ratios do not vanish asymptotically, they tend to $r_- = (25/70)e^{-4}$, and $r_- = (25/70)e^{-5}$, respectively. The third curve, shows, for comparison, the evolution of the ratio for the Λ CDM model, namely, $\rho_m/\rho_\Lambda = r_0 a^{-3}$ with an identical value for r_0 . Again, the interaction is seen to alleviate the coincidence problem.

bound on λ also ensures $Q > 0$.

Inserting (10) in (4) and assuming $w = -1$, we get

$$Q = \left(3 - \frac{\lambda a}{(1+a)^2} \right) H \frac{\rho_m}{1 + r_- e^{\lambda/(1+a)}}, \quad (11)$$

whence the corresponding differential equation for the DM density is

$$a \rho'_m + \left\{ 3 + \left[\frac{\lambda a}{(1+a)^2} - 3 \right] \frac{1}{1 + r_- e^{\lambda/(1+a)}} \right\} \rho_m = 0. \quad (12)$$

This has analytical solutions in the limiting cases, $a \rightarrow 0$ and $a \rightarrow \infty$; namely, $\rho_m \propto a^{-3r_+/(1+r_+)}$ and $\rho_m \propto a^{-3r_-/(1+r_-)}$, respectively, where $r_- = r_0 e^{-\lambda/2} > 0$; i.e., r never vanishes. Notice that, as in the previous case, the limiting solutions are rather reasonable; for small a , only a tiny amount of energy can be transferred to DM whence ρ_m decreased practically as though Q vanished, $\rho_m(a \ll 1) \sim a^{-3}$. For large a , a large amount of energy has already been transferred, significantly compensating the “natural” decrease of density; hence, $\rho_m(a \gg 1) \simeq \text{constant}$. This is apparent in Fig. 4, which depicts the numerical solution (12) for the cases $\lambda = 8$ (i.e., $r_- = (25/70) e^{-4}$), and $\lambda = 10$ [i.e., $r_- = (25/70) e^{-5}$], respectively.

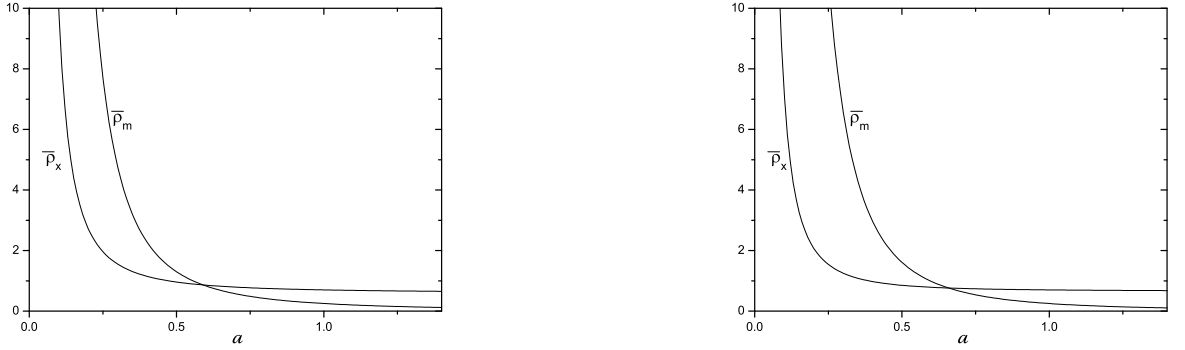


Figure 4: Left panel: Numerical solution to Eq. (12) in terms of the dimensionless quantity $\bar{\rho}_m \equiv \kappa \rho_m / (3H_0^2)$ with $\kappa \equiv 8\pi G$, for the choice $\lambda = 8$. Also shown is the curve of $\bar{\rho}_x = \bar{\rho}_m/r$. Right panel: The same but for the choice $\lambda = 10$.

C. Third parametrization

Similar to the previous one is

$$r = r_- \exp \left(\frac{\lambda}{(1+a)^2} \right), \quad (13)$$

where $\lambda > 0$ must be lower than $\simeq 10.125$ for Q to be positive and alleviate the coincidence problem. Here, $r_- = r_0 e^{-\lambda/4}$. Note that r_+ cannot be arbitrarily large because it fulfills $r_+ = r_0 e^{3\lambda/4}$.

Figure 5 depicts the ratio in terms of the scale factor for $\lambda = 8$ and $\lambda = 10$ as well as the corresponding plot for the Λ CDM model.

The interaction term in this case, with $w = -1$, reads

$$Q = \left(3 - \frac{2\lambda a}{(1+a)^3} \right) H \frac{\rho_m}{1 + r_- e^{\lambda/(1+a)^2}}. \quad (14)$$

Thus, the differential equation that governs the evolution of the DM energy density, assuming $w = -1$, reads

$$a \rho'_m + \left\{ 3 + \left[\frac{2\lambda a}{(1+a)^3} - 3 \right] \frac{1}{1 + r_- e^{\lambda/(1+a)^2}} \right\} \rho_m = 0. \quad (15)$$

In the limit situations $a \rightarrow 0$ and $a \rightarrow \infty$, one has $\rho_m \propto a^{-3r_+/(1+r_+)}$ and $\rho_m \propto a^{-3r_-/(1+r_-)}$, respectively. A plot of the numerical solution for $\lambda = 9.89$ is shown in Fig. 6.

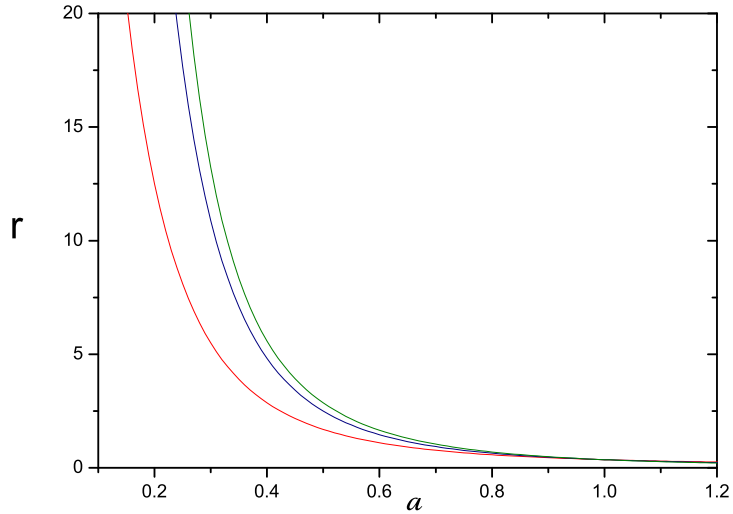


Figure 5: Plot of the ratio ρ_m/ρ_x as a function of the scale factor as given by Eq. (13). The first two curves from left to right are for $\lambda = 8$, $\lambda = 10$, respectively, with $r_0 = 25/70$. Also shown for comparison is the analogous curve for the Λ CDM model with the same value for r_0 .

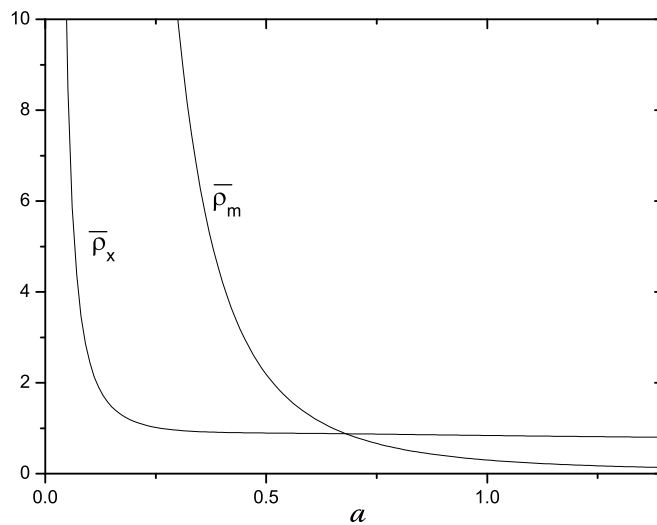


Figure 6: Numerical solution of Eq. (15) in terms of the dimensionless quantity $\bar{\rho}_m \equiv \kappa \rho_m / (3H_0^2)$ with $\kappa \equiv 8\pi G$ for the choice $\lambda = 9.89$ and $r_- = 0.031334$. Also shown is the corresponding curve of $\bar{\rho}_x$.

III. CONSTRAINING THE FREE PARAMETERS

Thus far, we did not resort to any specific theory of gravity. We have just used the FRW metric and the conservation equations (1)-(3). Accordingly, the parameters entering the above parametrizations have been left largely unconstrained. In order to most effectively restrict them one should use some gravity theory alongside the full set of

observational data of supernovae type Ia, baryon acoustic oscillations, history of the Hubble factor, cosmic microwave background, growth factor, and so on. However, this is beyond the scope of our work as we only aim to illustrate how reasonable expressions for Q can be obtained from the qualitative evolution of the ratio ρ_m/ρ_x . This is why we shall, for simplicity, assume $w = -1$ throughout and limit ourselves to quickly find acceptable values for the remaining parameters. This will be done by using Einstein gravity and the redshift at which the transition from decelerated to accelerated expansion took place.

Recently, Farooq and Ratra [18], based on 28 independent measurements of $H(z)$, determined with unprecedented accuracy that redshift, namely, $z_{da} = 0.74 \pm 0.05$ (1σ). The corresponding scale factor, $a_{da} = (1 + z_{da})^{-1}$, lies in the interval $0.56 \leq a_{da} \leq 0.59$, being 0.57 the central value.

From the deceleration parameter, $q = -\ddot{a}/aH^2$, and the Einstein field equations for a spatially flat universe,

$$H^2 = \frac{\kappa}{3} \rho, \quad \text{and} \quad \frac{\ddot{a}}{a} = -\frac{\kappa}{3} (\rho + 3p), \quad (16)$$

where $\rho = \rho_b + \rho_m + \rho_x$, $p = p_x = w\rho_x$, we obtain

$$q = \frac{1}{2} \left[\frac{[(\rho_{b0}/\rho_{m0}) + 1]r + 1 + 3w}{[(\rho_{b0}/\rho_{m0}) + 1]r + 1} \right]. \quad (17)$$

In the limiting cases $r \gg 1$ (i.e., $a \ll 1$, matter-dominated epoch) and $r \ll 1$ ($a \gg 1$, far future), one follows $q = 1/2$ and $q \rightarrow (1 + 3w)/2$, respectively, as it should. In the particular case $w = -1$, it reduces to

$$q = \frac{1}{2} \left(\frac{1.2r - 2}{1.2r + 1} \right), \quad (18)$$

where we have considered $\rho_{b0}/\rho_{m0} = 0.2$.

The latter expression of q together with the above value of a_{da} can be employed to get acceptable values for the free parameters in Eqs. (5), (10), and (13).

For the first parametrization Eq. (5), Fig. 7 depicts the dependence imposed on the parameters β and α by the observational constraint $q(a_{da}) = 0$. For simplicity we have taken $r_- = 0$.

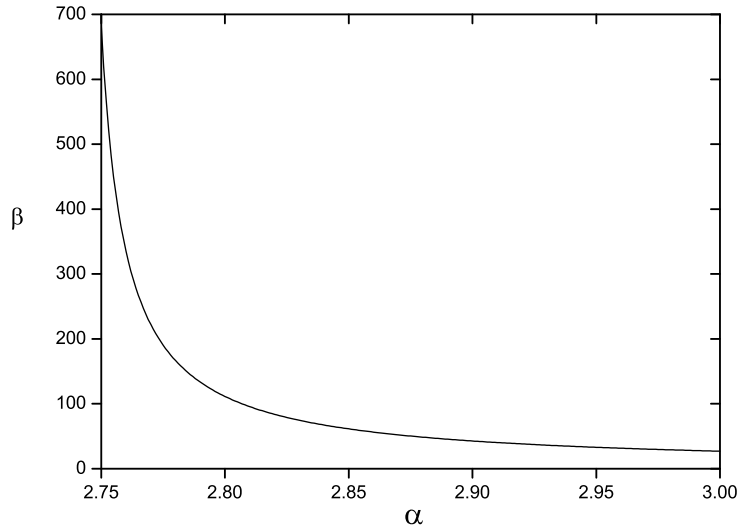


Figure 7: The parameter β in terms of α as imposed by the constraint $q(a = 0.57) = 0$ on the first parametrization, Eq. (5), with $r_- = 0$.

Then, the deceleration parameter vanishes at $a_{da} = 0.57$ for any point in the graph. Since we are dealing with the fixing of two parameters a further fixed point is necessary. We take the product $t_0 H_0$ where t_0 and H_0 stand for the age of the Universe and the Hubble constant, respectively. Measurements of the age of globular clusters and other old objects place the former in the interval $12 \lesssim t_0 \lesssim 14$ Gyr [19]. As for the latter, it is safe to say after the results of the Planck Collaboration [20], $H_0 = 67.3 \pm 1.2$ Km/s/Mpc, and the local measurements of Riess *et al* [21], $H_0 = 73.8 \pm 2.4$ Km/s/Mpc, that the said product must lie in the range $0.81 \lesssim t_0 H_0 \lesssim 1.09$. Here,

$$t_0 H_0 = \int_0^1 \frac{da}{a \sqrt{\Omega_{b0} a^{-3} + \Omega_{m0} f(a) + (1 - \Omega_{b0} - \Omega_{m0}) g(a)}}, \quad (19)$$

where $f(a) \equiv \rho_m/\rho_0$ is given by the right-hand side of Eq. (9) with $r_- = 0$ and $r_+ = r_0(1 + \beta)$, $g(a) \equiv \rho_x/\rho_{x0} = r_0 f(a)/r$, $\Omega_{b0} = 0.05$, and $\Omega_{m0} = 0.25$. Thus, only that pair of values (α, β) lying on the graph of Fig. 7 such that the corresponding product $t_0 H_0$ lies in the above interval can be considered for the parametrization. There is a further qualitative restriction. In order that dark energy does not spoil the standard picture of primeval nucleosynthesis it must be present only in a comparatively small amount at that epoch, namely, $\Omega_x < 0.045$ [16]. This implies that β must be large, no lower than, say, 50. At any rate, given the absence of a second strict observational constraint at the background level, there is a certain latitude in choosing the values of both parameters, i.e., properly speaking there is not a “best fit” as a handful pair of values (α, β) fits the data equally well. Thus, only after a substantial improvement on the observational estimation of H_0 and t_0 , it will be possible to determine the best fit. At any rate, for the sake of illustrating the method, we take $\alpha = 2.8$ and $\beta = 111.33$ (consequently, $r_+ \simeq 40.12$), and this corresponds to $t_0 H_0 \simeq 0.98$.

Likewise, for the second parametrization setting $q(a_{da}) = 0$ leads to $\lambda = 11.25$, thereby $r_- \simeq 0.0013$ and $r_+ \simeq 112$. Similarly, for the third parametrization one obtains $\lambda = 9.89$ whence $r_- \simeq 0.030$ and $r_+ \simeq 594$. As it can be numerically checked, the product $t_0 H_0$ yields 0.99 and 0.98 for the second and third parametrizations, respectively. Thus, in both cases it falls within the allowed range.

Figure 8 collects the evolution of the deceleration parameter for the three parametrizations [Eqs. (5), (10), and (13), respectively] for the above parameter values. Though not shown in the figure, $q(r_+) \simeq 0.46$ for the first one and $\simeq 0.49$ for the other two. Likewise, $q(r_-) \simeq -1$ for the two first parametrizations and $\simeq -0.95$ for the third one.

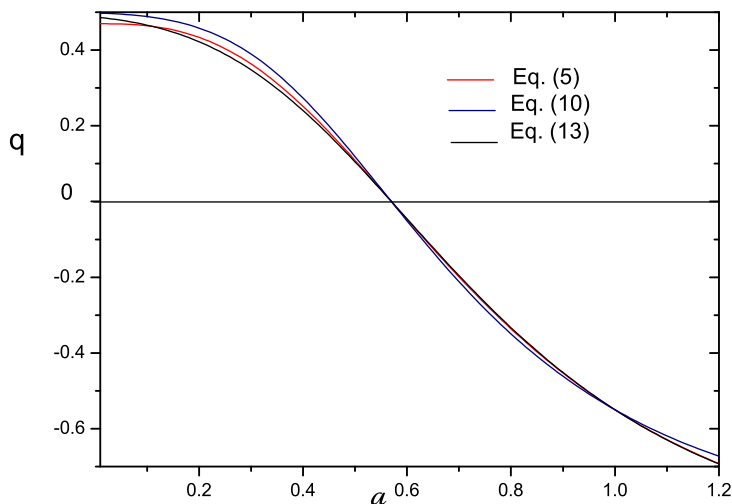


Figure 8: Evolution of the deceleration parameter in terms of the scale factor for the first, second and third parametrizations. In drawing the curves, we used $w = -1$, $r_0 = 25/70$, and $\rho_{b0}/\rho_{m0} = 0.2$.

To establish whether the above parametrizations, alongside the parameter values just obtained by imposing $q(a_{da}) = 0$, are acceptable —at least at a good qualitative level— we next determine $H(z)$ for each parametrization and contrast

it graphically with the history of the Hubble factor.
From the expressions $q = \ddot{a}/aH^2$ and $H = \dot{a}/a$, it follows

$$H = H_0 \exp \left\{ \int_0^z [1 + q(x)] d \ln(1+x) \right\}, \quad (20)$$

where H_0 is Hubble's constant. Expression (20) provides us with the Hubble history for every parametrization of ρ_m/ρ_x via the corresponding deceleration parameter.

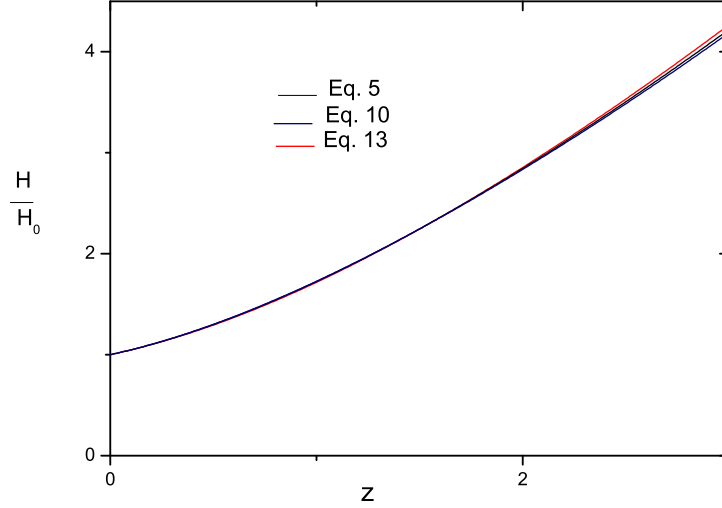


Figure 9: Hubble history corresponding to the three parametrizations, Eqs. (5), (10), and (13). For the curve corresponding to the first parametrization Eq. (5), we have assumed $\alpha = 2.5$ and $\beta = 697/3$, for the second parametrization Eq. (10), $\lambda = 8$, and for the third parametrization Eq. (13) $\lambda = 9.89$. In drawing the curves we have taken $w = -1$, $r_0 = 25/70$, and $\rho_{b0}/\rho_{m0} = 0.2$.

Figure 9 depicts the Hubble history (normalized to H_0) in the redshift interval $0 < z < 3$ for the three parametrizations: (5), (10), and (13). They begin to differ only after $z = 2$. Likewise, Figs. 10 and 11 show the ratio $H(z)/(1+z)$ for $0 < z < 24$, for the same three parametrizations confronted with the 28 observational $H(z)$ data collected in [18]. In Fig. 10 we have used $H_0 = 68 \text{ Km}/(\text{s} \cdot \text{Mpc})$ [22], a value within 1σ of the one reported by Ade *et al.*, namely, 67.3 ± 1.2 in the same units [20]. In Fig. 11, we used the central value $H_0 = 73.8 \text{ Km}/(\text{s} \cdot \text{Mpc})$, obtained by Riess *et al.* by local measurements [21]. The graph for the Λ CDM model is not shown because it essentially overlaps the other three.

A. The relative weight of Q

As mentioned in Sec. II, we do not expect the interaction term Q to be larger than the second term in the conservation equation for the DM energy density, Eq. (2). Then, assuming $w = -1$, every parametrization should fulfill

$$\zeta \equiv \frac{3\rho_m H}{Q} = \frac{3(1+r)}{3 + (a r'/r)} > 1. \quad (21)$$

This is satisfied by the three parametrizations —Eqs. (5), (10) and (13). For the first one, Fig. 12 illustrates (using the parameter values derived in the previous section) how the relative importance of Q , i.e., (ζ^{-1}) , increases with expansion and is bounded from above to be lower than unity (in fact, in this case, $\zeta \geq 15$ for the whole cosmic history). Notice that the graph is fully consistent with the fact that $|\rho'_m|$ is much larger for $a \ll 1$ than for a around

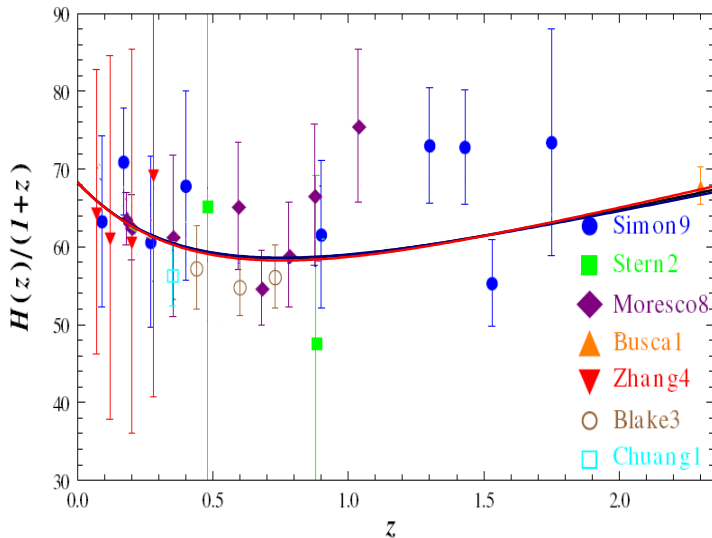


Figure 10: Plot of the ratio $H(z)/(1+z)$ assuming $H_0 = 68 \text{ Km}/(\text{s} \cdot \text{Mpc})$. Black, blue, and red lines correspond to the first, second and third parametrizations [Eqs. (5), (10), and (13)], respectively. The data error bars indicate 1σ confidence level. The $H(z)$ data were borrowed from Refs. [23] - [29].

and beyond unity (see Fig. 2).

A rather similar situation occurs for the second and third parametrizations [Eqs. (10) and (13)]. This is why we omit the corresponding graphs of ζ .

IV. TWO “POSSIBLE” DEGENERACIES

In principle, any given ratio $r(a)$ may be equally associated to two different scenarios; viz., the one considered so far (a nonvanishing interaction term Q with constant EOS w for the DE component) and also to the case of vanishing Q (no interaction) but with w given by a suitable EOS, different from the previous one. Therefore, one could not tell whether such a ratio points to the existence of an interaction or, perhaps, to a more involved EOS. In other words, a possible degeneracy between Q and w arises. Here, we shall argue that this degeneracy is only apparent because it can be readily broken at the background level since observable quantities, such as the Hubble factor and the deceleration parameter, significantly differ from one scenario to the other.

Indeed, by setting $Q = 0$ in the set of equations (1)–(3), the EOS that produces the same $r(a)$ as the one associated to a nonvanishing Q is easily found,

$$w(a) = -\frac{r'}{r} \frac{\rho'_m}{\rho_m}. \quad (22)$$

For illustrative purposes, let us focus on the second parametrization of r , namely, (10), and the corresponding

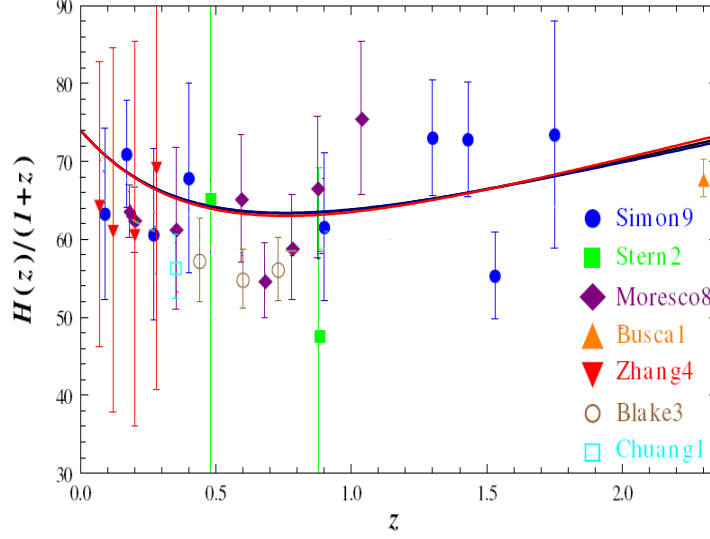


Figure 11: The same as Fig. 10 but using $H_0 = 73.8 \text{ Km}/(\text{s} \cdot \text{Mpc})$.

interaction term is given by (11). With the help of (12) we obtain

$$w(a) = -\frac{\lambda}{(1+a)^2} \frac{a}{3 + \left[\frac{\lambda a}{(1+a)^2} - 3 \right] \frac{1}{1+r_- e^{\lambda/(1+a)}}}. \quad (23)$$

Figure 13 depicts the dependence of w on the scale factor. This variable EOS produces the same $r(a)$ as the case with interaction, Eq. (11). However, this EOS seems to be at variance with observation because it contrasts with the findings of Serra *et al.* [30], who using a variety of observational data conclude that the EOS, varies, if at all, very little from $z = 1$ (i.e., $a = 0.5$) up to the present.

Let us consider the Hubble factor for the scenario with $Q = 0$ and the EOS (23),

$$\frac{H(a)}{H_0} = \sqrt{\Omega_{b0} a^{-3} + \Omega_{m0} a^{-3} + \Omega_{x0} \exp \left[-3 \int_1^a \frac{1+w(x)}{x} dx \right]}, \quad (24)$$

where $\Omega_{b0} = 0.05$, $\Omega_{m0} = 0.25$, and $\Omega_{x0} = 0.70$ are the current fractional densities of the various energy components.

Figure 14 depicts the evolution of the Hubble factor associated to Eq. (24) (solid line), and the one corresponding to interacting scenario with $w = -1$ (dashed line), both are normalized to H_0 . Both graphs depart more and more from each other as the scale factor decreases. Further, since $H(a)$ significantly differs between both models, the luminosity distance is also affected, as well as all other cosmological observable quantities (e.g., supernovae Ia brightness, age of the Universe, background acoustic oscillations, etc.). So, the degeneracy gets already broken at the background level.

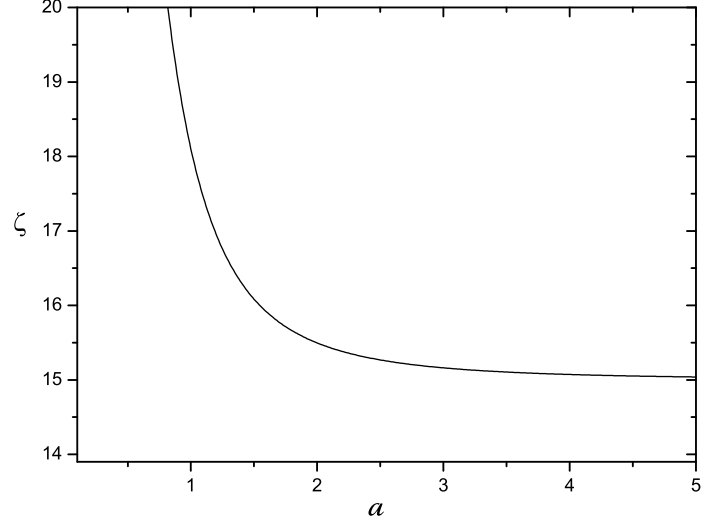


Figure 12: Evolution of the ratio (21) with expansion for the first parametrization, Eq. (5). The larger the scale factor, the smaller ζ . In drawing the curve we have used $r_0 = 25/70$, $\beta = 111.33$, and $\alpha = 2.8$.

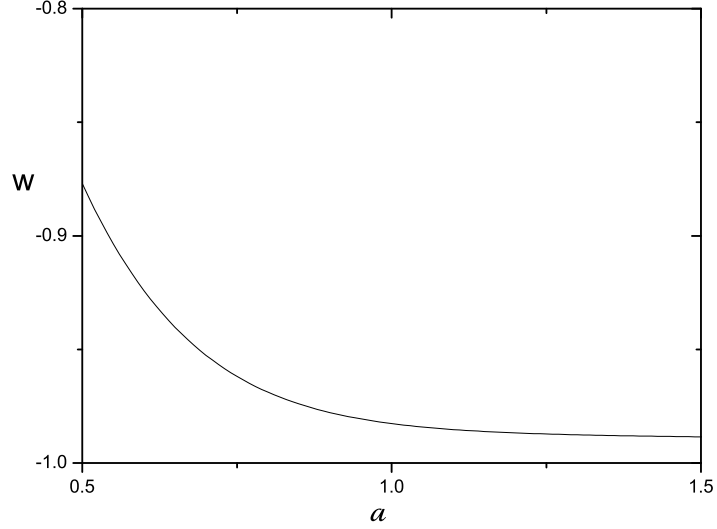


Figure 13: Evolution of the EOS corresponding to the second parametrization, Eq. (10), assuming $Q = 0$. In drawing the curve we have taken $\lambda = 11.25$ and $r_- = 0.0013$ (the best fit-values found above; see text).

The consideration of the deceleration parameter strengthens this point further. Equation (17) applies to both instances, viz., the model with $Q = 0$, and with r and w given by Eqs. (10) and (23), respectively, and the model with Q given by Eq. (11), where w is fixed to -1 . The observable q significantly varies from one model to the other because $w(a)$, which enters (17), does also, while all the other quantities in (17) are identical. Figure 15 makes this explicit. The difference is already significant, though not large, for $a = 0.57$ (the value observationally determined by Farooq and Ratra [18] at which q vanishes). For the $Q = 0$ model, $q(a = 0.57) \simeq 0.046$, while for the other model

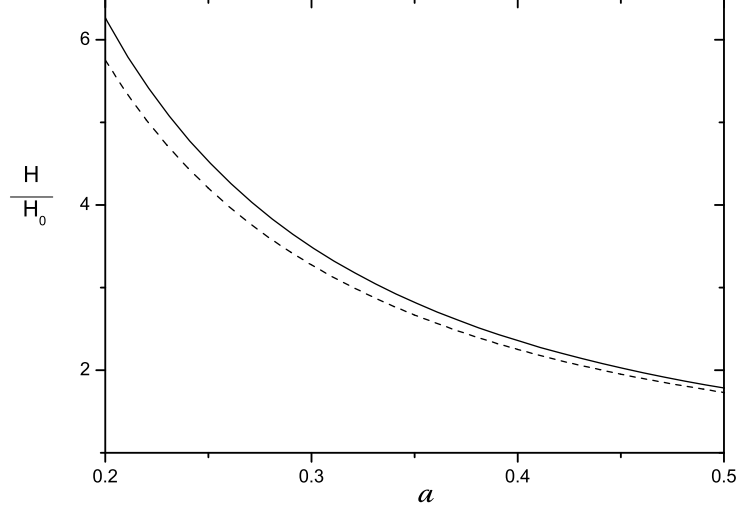


Figure 14: Evolution of the Hubble factor normalized to its present value, H_0 . The solid line corresponds to Eq. (24) with $w(a)$ given by (23). The dashed line depicts the Hubble factor associated to the case of the same $r(a)$ but with Q given by (11) and $w = -1$. In drawing both graphs we assumed $\Omega_{b0} = 0.05$, $\Omega_{m0} = 0.25$, $\Omega_{x0} = 1 - \Omega_{b0} - \Omega_{m0}$, $\lambda = 11.25$, and $r_- = 0.0013$.

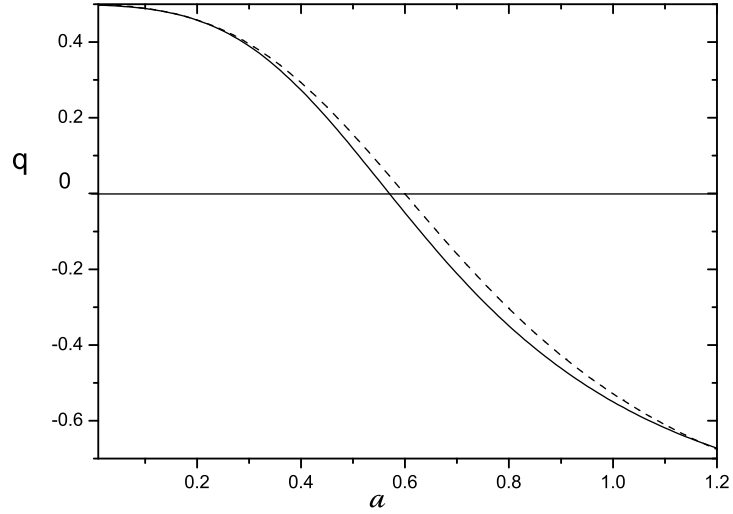


Figure 15: Evolution of the deceleration parameter for the model with $Q = 0$ (solid line) and for the model with Q given by (11) (dashed line). Both models share the same ratio r , equation (10), but their respective EOS are different -see text. In drawing the graphs we took $\rho_{b0}/\rho_{m0} = 0.2$, $\lambda = 11.25$, and $r_- = 0.0013$.

$q(a = 0.57) \simeq 0.0031$, with the former figure being about 15 times the latter. Again, the degeneracy is readily broken at the background level.

Here, we have just considered for illustrative purposes the interaction term associated to the second parametrization.

An identical conclusion can be attained for the other interaction terms above.

Another apparent degeneracy is as follows. In principle, one could think that it would be possible to reproduce the same expansion history $H(z)$ and, consequently, the same deceleration parameter $q(z)$ in a noninteracting scenario ($Q = 0$) by using a suitably tailored EOS $w(z)$, for the dark energy component in an interacting scenario ($Q \neq 0$) with $w = \text{constant}$. Obviously, now the ratio $r(z)$ will differ from one scenario to the other. Since $H(z)$ is the same in both, they will share the same luminosity and angular distances whence the models will be indistinguishable at the background level.

However, as we will see, this possibility does not exist in general, nor does it exist in the particular cases of the three parametrizations above or for parametrizations (30) and (32) considered below. Indeed, by equating the right-hand sides of Friedmann's equation for spatially flat universes corresponding to the interacting model, and assuming $w = -1$ (for simplicity), with the noninteracting one $Q = 0$ but with an undetermined EOS $w(a)$, it follows that the latter quantity is given implicitly by the expression

$$\int_a^1 \frac{1 + w(a)}{a} da = \frac{1}{3} \ln \{ r_0 [f(a) - a^{-3}] + g(a) \}, \quad (25)$$

where $f(a)$ stands for the DM ratio $\rho_m(a)/\rho_{m0}$ in the interacting model [e.g. by the right-hand side of Eq. (9) in the case of the first parametrization] and $g(a) \equiv \rho_x/\rho_{x0} = r_0 f(a)/r(a)$. In writing Eq. (25), we bore in mind that the current fractional densities of the three components coincide in both models.

Because of at any $a < 1$, the amount of DM in the interacting model is necessarily less than in the case of vanishing Q (in which instance the DM density would obey $\rho_m = \rho_{m0} a^{-3}$), one follows $f(a) < a^{-3}$, and the curly brackets on the right hand-side of (25) can be negative in some interval of the scale factor when $a < 1$. This severely constrains $w(a)$ since the said brackets must be non-negative for any value of a if $w(a)$ is to exist at all. Accordingly, if the function

$$\chi(a) \equiv f(a) - a^{-3} + \frac{f(a)}{r(a)} \quad (26)$$

takes negative values in some interval of the scale factor, there will be no $w(a)$ capable of reproducing the $H(a)$ function of a given interacting model. This is the case of the three parametrizations (5), (10), and (13), as Figs. 16 and 17 illustrate.

As Fig. 18 shows, the same is true for the parametrizations given by Eqs. (30) and (32) (see below). These correspond to the widely used interaction terms $Q = \xi H \rho_m$ and $Q = \xi H \rho_x$, respectively. Here, ξ is a semipositive, small, constant parameter.

In general, it is reasonable to expect that for any $Q > 0$ interaction the $f(a)$ function may be “piecewise” expressed as $f(a) = a^{-3+\epsilon}$ with $0 < \epsilon \ll 1$ a constant parameter in every small-scale factor interval but such that it slightly varies between two neighboring intervals; the smaller the interval, the better the approximation is. Then, the expression

$$\chi(a) \simeq a^{-3} \left[a^\epsilon \left(1 + \frac{1}{r(a)} \right) - 1 \right] \quad (27)$$

will be valid in every small interval of the scale factor. Accordingly, bearing in mind that $dr(a)/da < 0$, and that for $r \gtrsim (0.25/0.70)^{1/3} \simeq 0.71$, DM dominates over DE (otherwise, the large-scale structure we observe today could not be accounted for), it follows that $r(a) > 1$ for a small enough. Then, for some scale factor, say $a_* < 1$, $\chi(a)$ will be negative in the interval $0 < a < a_*$, and no EOS $w(a)$ will exist such that the corresponding non-interacting model can reproduce the same history of the Hubble function of a given interacting model with constant w .

On the other hand, even wildly assuming the existence of such EOS, both kinds of models will be readily told apart at the perturbative level without the need to perform a detailed analysis. Indeed, because in the interacting model DM is continuously added to that component from the DE (recall that $Q > 0$), as mentioned above, the amount of dark matter in the past was necessarily less than in noninteracting scenarios at the same redshift. This is illustrated by Fig. 19 where the ratio $\eta \equiv \rho_m(z)/\rho_{m0} (1+z)^3$ vs. z is depicted for the case of the second parametrization, Eq. (10), in the redshift interval $0 \leq z \leq 20$. On the other hand, since the present amount of matter (baryonic, Ω_{b0} and

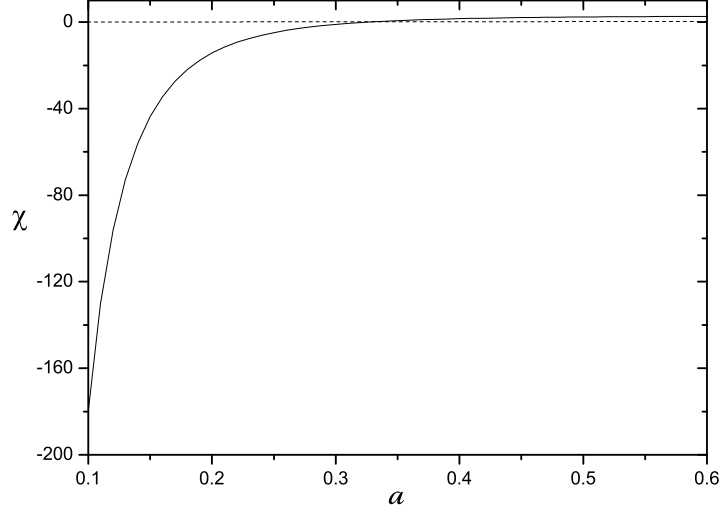


Figure 16: Evolution of function χ , Eq. (26), in terms of the scale factor for the case of the first parametrization, Eq. (5). As is apparent, $\chi > 0$ only for $a > 0.4$, thereby no EOS of any noninteracting model can reproduce the Hubble history, $H(z)$, of the model corresponding to the first parametrization. In plotting the graph we have used $\Omega_{b0} = 0.05$, $\Omega_{m0} = 0.25$, $r_- = 0$, $r_+ = 40.12$, $\alpha = 2.8$, and $\beta = 111.33$.

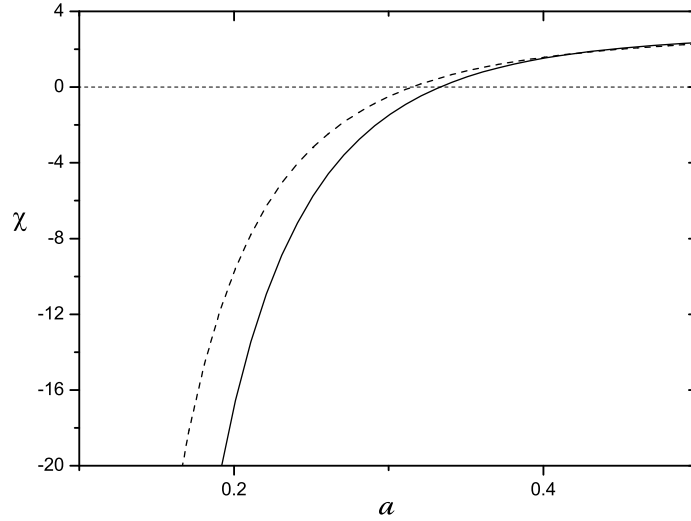


Figure 17: Solid line: Evolution of function χ , Eq. (26), in terms of the scale factor for the case of the second parametrization, Eq. (10). Dashed line: The same but for the third parametrization, Eq. (13). As is seen, $\chi(a \lesssim 0.32) < 0$ and $\chi(a \lesssim 0.30) < 0$ for the second and third parametrizations, respectively. In drawing the graphs we have used the value of the parameter λ that best fits the observational data [$q(a = 0.57) = 0$], i.e., 11.25 and 9.89 for the second and third parametrizations, respectively. In both cases we have assumed $\Omega_{b0} = 0.05$ and $\Omega_{m0} = 0.25$.

dark Ω_{m0}) has to be the same in both models, the growth function, $f_g = d \ln D_+ / d \ln a$ in the interacting scenario

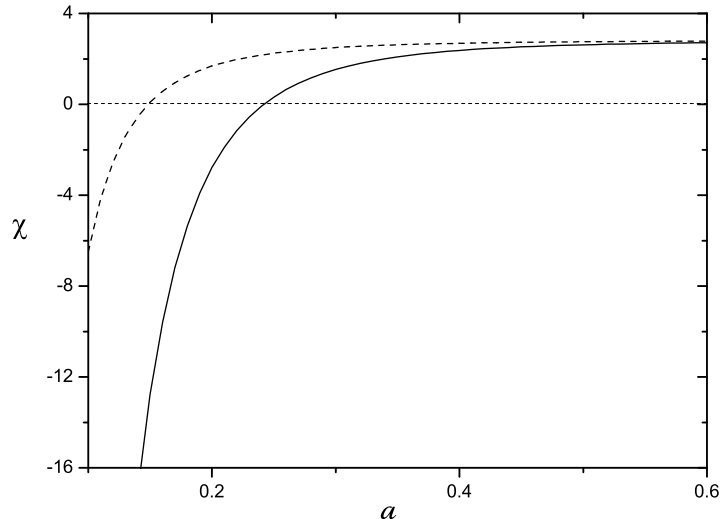


Figure 18: Solid line: Evolution of function χ , Eq. (26), in terms of the scale factor for the case of parametrization (30). Dashed line: The same but for parametrization (32). For both parametrizations χ is negative in a considerable interval of the scale factor. In drawing the graphs we have considered $r_0 = 0.25/0.70$, $w = -1$, and $\xi = 0.01$. In both cases we have assumed $\Omega_{b0} = 0.05$ and $\Omega_{m0} = 0.25$.

must be larger at any redshift than in the Λ CDM model, while the same function in the noninteracting scenario will be, at most, as large as in the latter model. While current measurements of $f_g(z)$ are not accurate enough to do the job, future measurements —possibly the next generation of data—will, hopefully, be precise enough to discriminate between the said scenarios. This may well be achieved by the Euclid mission [31]. Thanks to the latter, $f_g(z)$ is expected to be determined with an accuracy between 1% and 2.5% in the redshift interval $0.5 < z < 2$ (see Figs. 2 and 3 in Di Porto *et al.* [32] and Figs. 14 and 15 in Amendola *et al.* [33]). In summary, if, by any chance, an interacting model and noninteracting one happen to share an identical expansion history, in order to tell one model from the other, it will suffice to see whether the experimentally determined growth function lies above or below the theoretical growth function of the Λ CDM model. If it lies below, the interacting model gets automatically discarded; if it lies above it is the noninteracting one that should be disposed of. Altogether, sooner or later observational data will constrain $f_g(z)$ sufficiently enough so that without explicit calculating the said function for any of the two kind of models it will be possible to discriminate one from the other with full certainty.

Likewise, the maximum of the matter power spectrum of interacting models will be shifted to larger scales with respect noninteracting models. Indeed, the redshift of matter-radiation equality z_{eq} determines when subhorizon density perturbations start to grow. A model with a larger fraction of DM (i.e., a noninteracting one) will reach this equality earlier than a model with a smaller fraction of DM (an interacting model with $Q > 0$). The power spectrum of matter density perturbations has its maximum at $k = 2\pi/d_H(z_{eq})$, where $d_H(z)$ is the radius of the horizon at redshift z . In any model, when $\Omega_m + \Omega_b = \Omega_{rad}(1 + z_{eq})$ the perturbations start to grow. Because of the Meszaros effect [34], the lower the fraction of DM, the later the growth of density perturbations will commence, making the models differ further. Eventually, data coming from large-scale structure observations will render this distinction feasible.

V. SOME PROPOSED INTERACTION TERMS

As mentioned in the Introduction, several interaction terms have been proposed in the literature over the years, all of them —due to our lack of knowledge of the dark sector at the fundamental level— were based just on heuristic arguments and mathematical simplicity.

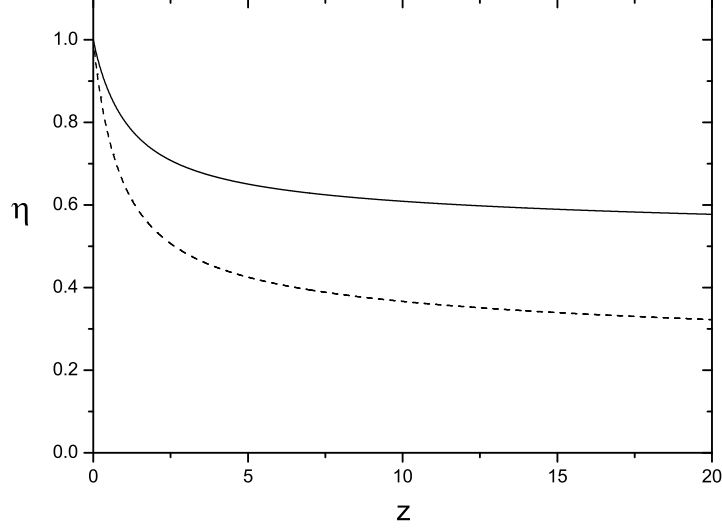


Figure 19: Evolution of the ratio $\eta \equiv \rho_m(z)/\rho_{m0}(1+z)^3$, where $\rho_m(z)$ is the dark matter density in the case of the second parametrization. The solid line corresponds to $\lambda = 10$, the dashed one to $\lambda = 8$. In drawing both curves $r_0 = 25/70$ was assumed.

Here we will focus on two sets on interaction terms. The first set is [10, 35],

$$Q = \xi H \rho_m, \quad Q = \xi H \rho_x, \quad Q = \xi H (\rho_m + \rho_x), \quad Q = \xi H \frac{\rho_m \rho_x}{\rho_m + \rho_x}, \quad Q = -\xi (\rho_m + \rho_x), \quad (28)$$

where ξ , stands for a constant and small, $|\xi| \ll 1$, dimensionless parameter.

A second set, given by [36]

$$Q = \Gamma \rho_m, \quad Q = \Gamma \rho_x, \quad \text{and} \quad Q = \Gamma (\rho_m + \rho_x), \quad (29)$$

where the constant Γ has the dimensions of inverse of time and was inspired by proposals about the curvaton decay [37] and the decay of DM into relativistic particles [38].

By equating the right hand-sides of (4) and (28.1) and integrating the resulting expression, with $w = \text{constant}$, one obtains

$$r = \frac{(1+c)r_0 a^{\xi(1+c)}}{1+c+r_0 - r_0 a^{\xi(1+c)}}, \quad (30)$$

where $c \equiv 3w/\xi$.

As it can be readily checked, for $0 < \xi \ll 1$, r is non-negative for any value of the scale factor, see Fig. 20. Further, it does not diverge when $a \rightarrow 0$; in fact $r_+ = -(1+c) > 0$. This is apparent in the left panel of Fig.1 of Ferreira *et al.* [39].

For $\xi < 0$ satisfying $|\xi| \ll 1$, r takes negative values and diverges when $a = a_*$ with

$$a_* = \left(\frac{r_0}{1+c+r_0} \right)^{|\xi|(1+c)} < 1. \quad (31)$$

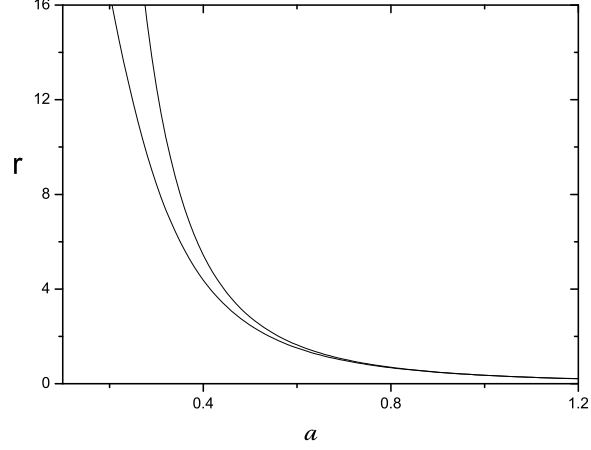


Figure 20: Evolution of ρ_m/ρ_x for $\xi = 0.1$ and $\xi = 0.01$, according to Eq. (30). In drawing the curves we have assumed $w = -1$ and $r_0 = 25/70$. These overlap for $a \geq 0.75$.

Proceeding along parallel lines with the second interaction term, Eq. (28.2), one follows

$$r = \frac{[(1+c)r_0 + 1] a^{\xi(1+c)} - 1}{1+c}. \quad (32)$$

As in the previous case, for $0 < \xi \ll 1$, r is non-negative for any value of the scale factor, see Fig. 21. By contrast,

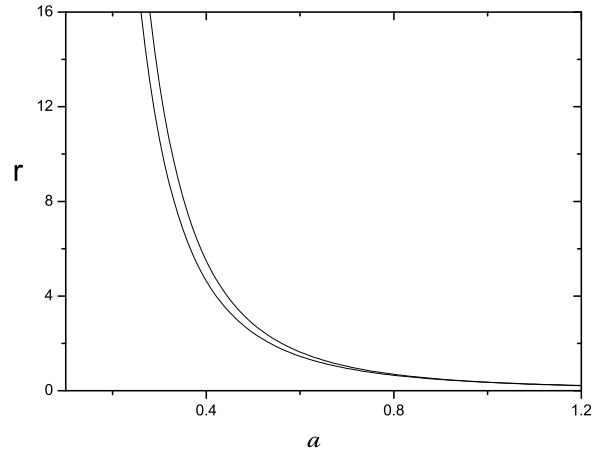


Figure 21: The same as Fig. 20 but for Eq. (32).

for $\xi < 0$, with $|\xi| \ll 1$, it becomes negative for $a > a_* = [1 + r_0(1+c)]^{1/|\xi|(1+c)} > 1$. Further, regardless of the sign of ξ , r_+ diverges (see middle panel of Fig. 1 in [39]).

From Eqs. (4) and (28.3), one is led to

$$\frac{dr}{r^2 + (2+c)r + 1} = \xi \frac{da}{a}. \quad (33)$$

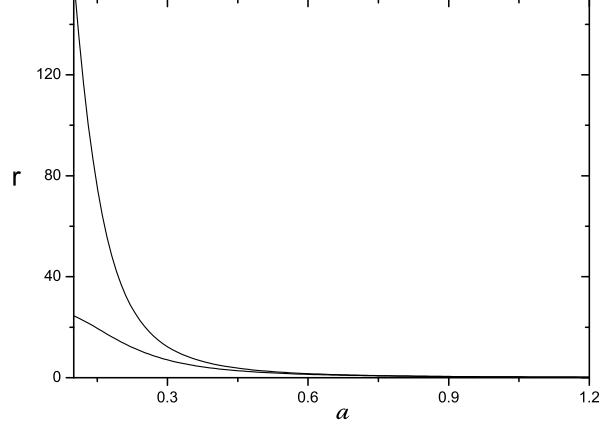


Figure 22: Two numerical solutions to (33). The lower and upper curves correspond to $\xi = 0.1$ and $\xi = 0.01$, respectively. In drawing the curves we have taken $r_0 = 25/70$ and $w = -1$.

Two numerical solutions to this equation are depicted in Fig. 22. Though not shown, r remains finite in the $a \rightarrow 0$ limit. In fact, $r_+ = (2/3\xi) - 1 + \sqrt{(9/4\xi^2) - (3/\xi)}$, as is apparent in the right panel of Fig. 1 of [39] and in Fig. 2 of Olivares *et al.* [40].

For the interaction term given by Eq. (28.4) one obtains

$$r \left(r + \frac{1+c}{c} \right)^{1/c} = r_0 \left(r_0 + \frac{1+c}{c} \right)^{1/c} a^{\xi(1+c)}. \quad (34)$$

Figure 23 shows the behavior of r for $\xi = 0.1$ and $\xi = 0.01$. Both graphs essentially overlap; on the other hand, there would have been practically no difference if we would have used $\xi = -0.1$ and $\xi = -0.01$ instead. In this case r_+ diverges for any sign of ξ . This is consistent with the fact that (28.4) reduces to (28.2) when $\rho_m \gg \rho_x$; i.e., when $a \rightarrow 0$.

Let us consider now the interaction term (28.5). With the help of the conservation equations (2) and (3), it can be cast as

$$Q = 3\xi H \rho_m \frac{1+r+w}{r}. \quad (35)$$

Following the same steps as before, we find

$$\frac{dr}{\xi(1+r)^2 + wr(1+\xi) + \xi w} = 3 \frac{da}{a}. \quad (36)$$

This equation integrates to

$$a = \exp [F(r) - F(r_0)], \quad (37)$$

where

$$F(r) = \frac{2}{3\sqrt{|w|}\sqrt{(1+\xi)^2|w|-4\xi}} \tanh^{-1} \left[\frac{(1+\xi)|w|-2\xi(1+r)}{\sqrt{|w|}\sqrt{(1+\xi)^2|w|-4\xi}} \right]. \quad (38)$$

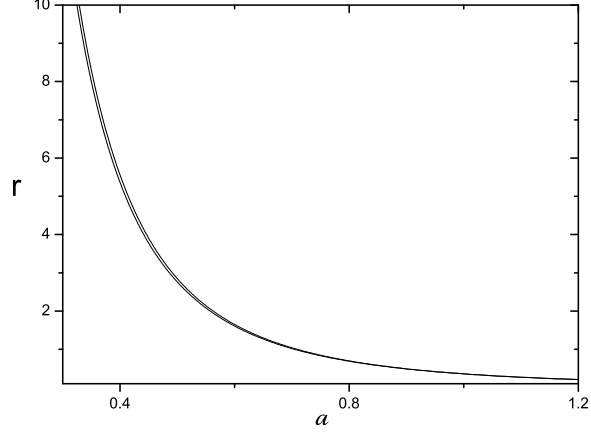


Figure 23: Evolution of the ratio ρ_m/ρ_x vs the scale factor, according to (34), for $\xi = 0.1$ and $\xi = 0.01$. In drawing the curves we have assumed $r_0 = 25/70$ and $w = -1$.

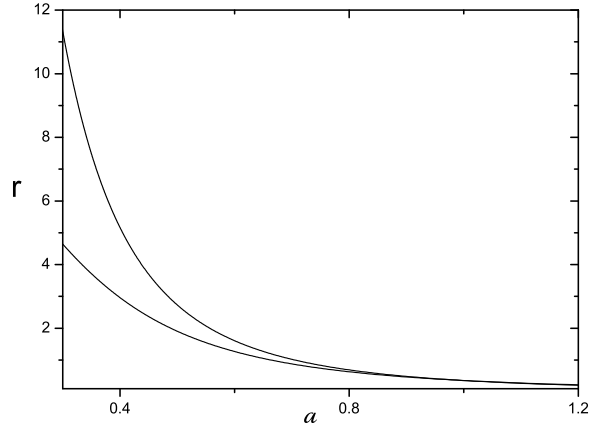


Figure 24: Ratio ρ_m/ρ_x vs the scale factor according to Eq. (37). The upper and lower curves correspond to $\xi = 0.1$ and $\xi = 0.01$. In drawing the curves we have used $r_0 = 25/70$ and $w = -1$.

Figure 24 shows the evolution of $r(a)$ for $\xi = 0.1$ and $\xi = 0.01$. In this case, r_+ remains finite, and for $w = -1$, it reads

$$r_+ = \frac{(1 - \xi) + \sqrt{(1 + \xi)^2 - 4\xi}}{2\xi}. \quad (39)$$

Obviously, ξ cannot be negative.

Altogether, the interactions terms given by Eqs. (28.1), (28.3), and (28.5) fulfill the criteria of Sec. II provided $\xi > 0$; not so the other two since r_+ diverges.

As for the interaction term given by Eq. (29.1), we proceed as follows. Let $\Gamma = \gamma H_0$, where γ denotes a dimensionless constant. Next, we equate the right-hand side of the resulting expression for Q with the corresponding one of (4).

After simplifying and introducing the ansatz $H = H_0 r^\alpha$ (piecewise valid for $\alpha = \text{constant}$ in the range $0 < \alpha < 1$), we arrive at

$$\frac{dr}{3wr + \gamma r^{1-\alpha}(1+r)} = \frac{da}{a}. \quad (40)$$

It is seen that dr/da will be negative in general only if $\gamma < 0$. However, as the left panel of Fig. 1 in [39] suggests, r_+ diverges.

A similar situation occurs for the interaction terms (29.2) and (29.3). Thus, we infer that the three expressions for Q in (29) fail as physically acceptable interaction terms in the dark sector.

VI. CONCLUDING REMARKS

Ideally speaking, any valid expression for the interaction between the DM and DE components could be obtained by writing the equations of motion after varying the corresponding Lagrangian. However, one cannot propose such Lagrangian expression without, implicitly or explicitly, presuming a good deal about the microscopic nature of these components. Worse than that, as recently noted, because two fluids should not be considered ideal on their own if they interact with one another, it is unclear if Lagrangian (even if is just effective) could be ascribed to such a situation [41]. This is why we have followed a diverse route when looking for phenomenological, but useful, expressions of the said interaction term.

Any interaction in the dark sector is bound to change the ratio between the energy densities of DM and DE with respect to the very particular case of no interaction, as it is directly connected to it [see Eq. (4)]. Thus, in Sec. II, by parametrizing this ratio on simple, sensible grounds, reasonable expressions for Q follow, as Eqs. (8), (11), and (14) illustrate. Here we wish to stress that this method rests solely on the FRW metric and the energy conservation equations and not on any specific cosmological model or theory of gravity. (Obviously, other expressions for Q differing from the ones proposed here in Sec. II are obtainable using other possible parametrizations of ρ_m/ρ_x .) Likewise, we have restricted ourselves to the case $Q > 0$ because this helps alleviate the coincidence problem.

Useful constraints on the free parameters have been readily obtained (Sec. III) by imposing the vanishing of the deceleration parameter at the transition redshift $z_{da} = 0.74 \pm 0.05$, as recently determined [18]. Admittedly, the latter implies the use of one or another theory of gravity—in the present case, general relativity. At any rate, the above parametrizations seem to comfortably reproduce the history of the Hubble factor (see Figs. 10 and 11) which suggests that these terms should behave reasonably well at the background level because in FRW universes, $H(z)$ is directly connected to the luminosity and angular distances. Therefore, they are expected to make good fits to current cosmological data from supernovae type Ia, baryon acoustic oscillations, the shift of the first acoustic peak of the cosmic microwave background temperature spectrum, and gas mass fraction in galaxy clusters. Nevertheless, we do not claim that these interaction terms should be taken too seriously since they were proposed mainly on illustrative purposes and, ultimately, any cosmological model that assumed whatever interaction term must also fit observations at the perturbation level, such as the matter power spectrum and the evolution of the matter growth factor; but this lies beyond the scope of this paper and will be the subject of a future research.

We wish to stress that the $r(a)$ expressions based on the criteria laid down in Sec. II do not necessarily converge to the Λ CDM ratio $r_\Lambda \propto a^{-3}$ at any limit. This is so because r_Λ diverges very rapidly for $a \rightarrow 0$, which contrasts with the condition that $r(a)$ varies very little or remains constant at very early times. Nevertheless, by suitably adjusting their free parameters, they can approximate r_Λ for $a \gtrsim 0.1$ with great accuracy.

As Sec. IV illustrates, the possible degeneracies between the interaction term and the EOS of DE are only apparent because they can be readily broken at the background and perturbative levels. Specifically, noninteracting models are unable to reproduce the same history of the Hubble function of a interacting model (and vice versa).

Finally, for the sake of completeness, in Sec. V the ratio ρ_m/ρ_x associated to a handful of interaction terms found in the literature has been analyzed. Some of them happen to satisfy the reasonable criteria laid down in Sec. II.

Acknowledgments

We are indebted to Fernando Atrio-Barandela and Enrique Gaztañaga for helpful conversations. SdC and RH were supported by the COMISION NACIONAL DE CIENCIAS Y TECNOLOGIA through FONDECYT Grant N^os 1110230 and 1130628. SdC was partially supported by PUCV Grant N^o 123.710 and RH by DI-PUCV N^o 123724. D.P. is indebted to the “Instituto de Física de la Pontificia Universidad Católica de Valparaíso”, where part of this work was done, for warm hospitality and financial support. This research was partially supported by the “Ministerio de Economía y Competitividad, Dirección General de Investigación Científica y Técnica”, Grant N^o. FIS2012-32099. Sadly, shortly after this paper was completed Prof. Sergio del Campo, unexpectedly, passed away. RH and DP dedicate this paper to his Memory.

-
- [1] A.M. Polyakov, Nucl. Phys. B 797, 199 (2008).
 - [2] A.M. Polyakov, Nucl. Phys. B 834, 316 (2010).
 - [3] D. Krotov and A.M. Polyakov, Nucl. Phys. B 849, 410 (2011).
 - [4] Ph. Brax and J. Martin, J. Cosmol. Astropart. Phys. 11 (2006) 008.
 - [5] J. Martin (private communication).
 - [6] P.J. Steinhardt, in *Critical Problems in Physics*, edited by V.L. Fitch and D.R. Marlow (Princeton University Press, Princeton, NJ, 1997).
 - [7] Germán Olivares, Fernando Atrio-Barandela, and Diego Pavón, Phys. Rev. D 77, 103520 (2008).
 - [8] A.A. Costa, X-D. Xu, B. Wang, E.G.M. Ferreira, and E. Abdalla, Phys. Rev. D 89, 103531 (2014).
 - [9] E. Abdalla, E.G.M. Ferreira, J. Quintin, and B. Wang, arXiv:1412.2777.
 - [10] Yu. L. Bolotin, A. Kostenko, O.A. Lemets, and D.A. Yerokhin, Int. J. Mod. Phys. D 24, 1530007 (2015).
 - [11] Fernando Atrio-Barandela and Diego Pavón, in *Dark Energy — Current Advances and Ideas*, edited by J. R. Choi (Research Singpost, Trivandrum, India, 2009).
 - [12] C. Skordis, A. Pourtsidou, and E.J. Copeland, Phys. Rev. D 91, 083537 (2015).
 - [13] J. Gleyzes, D. Langlois, M. Mancarella, and F. Vernizzi, arXiv:1504.05481.
 - [14] P.J.E. Peebles and B. Ratra, Rev. Mod. Phys. 75, 559 (2003).
 - [15] K. Hagiwara *et al.*, Phys. Rev. D. 66, 010001 (2002).
 - [16] R. Bean, S. H. Hansen, and A. Melchiorri, Phys. Rev. D 64, 103508 (2001).
 - [17] J.-Q. Xia and M. Viel, J. Cosmol. Astropart. Phys. 04 (2009) 002.
 - [18] O. Farooq and B. Ratra, Astrophys. J. 766, L7 (2013).
 - [19] B. Chaboyer, Phys. Rep. 307, 23 (1998); F.D. Grundahl *et al.*, Astron. J. 120, 1884 (2000); R. Caryl *et al.*, Nature (London) 409, 691 (2001).
 - [20] P.A.R. Ade *et al.* (Planck Collaboration), Astron. Astrophys. 571, A16 (2014).
 - [21] A.G. Riess *et al.*, Astrophys. J. 730, 119 (2011).
 - [22] G. Chen, J.R. Got III, and B. Ratra, Publ. Astron. Soc. Pac. 115, 1269 (2003).
 - [23] N.G. Busca *et al.*, Astron. Astrophys. 552, A96 (2013).
 - [24] C. Blake, S. Brough, M. Colless, *et al.*, Mon. Not. R. Astron. Soc. 425, 405 (2012).
 - [25] C.H. Chuang, and Y. Wang, Mon. Not. R. Astron. Soc. 435, 255 (2013).
 - [26] M. Moresco, A. Cimatti, R. Jimenez *et al.*, J. Cosmol. Astropart. Phys. 08 (20012) 006.
 - [27] J. Simon, L. Verde, and R. Jimenez, Phys. Rev. D 71, 123001 (2005).
 - [28] D. Stern, R. Jimenez, L. Verde, M. Kamionkowski, and S.A. Stanford, J. Cosmol. Astropart. Phys. 02 (2010) 008.
 - [29] C. Zhang, H. Zhang, S. Yuan, T.-Jie Zhang, and Y.-C. Sun, Res. Astron. Astrophys. 14, 1221 (2014).
 - [30] P. Serra *et al.*, Phys. Rev. D 80, 121302(R) (2009).
 - [31] <http://www.euclid-ec.org>.
 - [32] E. Di Porto, L. Amendola, and E. Branchini, Mon. Not. R. Astron. Soc. 419, 985 (2012).
 - [33] L. Amendola *et al.*, Living Rev. Relativity 16, 6 (2013).
 - [34] P. Mészáros, Astron. Astrophys. 37, 225 (1974).
 - [35] I.E. Sánchez, Gen. Relativ. Gravit. 46, 1769 (2014).
 - [36] G. Caldera-Cabral, R. Maartens, and L.A. Ureña-López, Phys. Rev. D 79, 063518 (2009).
 - [37] K. A. Malik, D. Wands, and C. Ungarelli, Phys. Rev. D 67, 063516 (2003).
 - [38] R. Cen, Astrophys. J. 546, L77 (2001).
 - [39] Pedro C. Ferreira, Diego Pavón, and Joel C. Carvalho, Phys. Rev. D 88, 083503 (2013).
 - [40] Germán Olivares, Fernando Atrio-Barandela, and Diego Pavón, Phys. Rev. D 71, 063523 (2005).
 - [41] V. Faraoni, J.B. Dent, and E.N. Saridakis, Phys. Rev. D 90, 063510 (2014).